

Parameter-uniform numerical methods for singularly perturbed linear transport problems

José Luis Gracia¹  | Adrian Navas-Montilla²  | Eugene O'Riordan³ 

¹IUMA and Department of Applied Mathematics, University of Zaragoza, Zaragoza, Spain

²I3A and Fluid Mechanics Department, University of Zaragoza, Zaragoza, Spain

³School of Mathematical Sciences, Dublin City University, Dublin, Ireland

Correspondence

José Luis Gracia, IUMA and Department of Applied Mathematics, University of Zaragoza, Zaragoza, Spain.

Email: jlgracia@unizar.es

Communicated by: X. Wang

Funding information

Diputacion General de Aragon (E24-17R); Institute of Mathematics and Applications (IUMA); Ministerio de Ciencia e Innovación, Grant/Award Number: PGC2018-094341-B-I00 and PID2019-105979GB-I00

Pointwise accurate numerical methods are constructed and analysed for three classes of singularly perturbed first order transport problems. The methods involve piecewise-uniform Shishkin meshes and the numerical approximations are shown to be parameter-uniformly convergent in the maximum norm. A transport problem from the modelling of fluid–particle interaction is formulated and used as a test problem for these numerical methods. Numerical results are presented to illustrate the performance of the numerical methods and to confirm the theoretical error bounds established in the paper.

KEYWORDS

fluid particle interaction, Shishkin mesh, singularly perturbed, transport equation

MSC CLASSIFICATION

65M15, 65M12

1 | INTRODUCTION

Mathematical models of flow related physical problems (e.g., semiconductor devices,¹ Chapter³ plasma sheath formation² or fluid-particle interaction^{3–5}) typically involve coupled systems of three or more partial differential equations. Transport equations of the form $u_t + \nabla f(u) = g(x, t)$ often appear in one or more of the equations within these systems. In many cases, the flow is convection-dominated and steep gradients appear in certain subregions of the domain. These problems are singularly perturbed problems. Our interest lies in designing parameter-uniform numerical methods⁶ for a wide class of singularly perturbed problems. These numerical methods are designed to generate globally pointwise accurate approximations to the solutions and the order of convergence is retained irrespective of the value of the singular perturbation parameter. In this article, we study singularly perturbed problems arising in linear transport problems of the form $u_t + au_x + bu = f$.

Shishkin⁷ examined singularly perturbed transport problems of the form: Find $u(x, t) \in C^2(\bar{\Omega})$, $\Omega := (0, L] \times (0, T]$ such that

$$\begin{aligned} u_t + \varepsilon au_x + bu &= f(x, t), (x, t) \in \Omega; \\ u(x, t) &\text{ given for } (x, t) \in \partial\Omega := \bar{\Omega} \setminus \Omega, a > 0, b \geq 0, (x, t) \in \bar{\Omega}. \end{aligned}$$

The parameter $0 < \varepsilon \leq 1$ can be arbitrarily small in size. As $\varepsilon \rightarrow 0$, the characteristic curves (associated with this first order problem) tend towards vertical lines of the form $x = x_0$. A boundary layer of order $O(\varepsilon)$ will appear near the edge

This is an open access article under the terms of the Creative Commons Attribution-NonCommercial-NoDerivs License, which permits use and distribution in any medium, provided the original work is properly cited, the use is non-commercial and no modifications or adaptations are made.

© 2022 The Authors. Mathematical Methods in the Applied Sciences published by John Wiley & Sons, Ltd.

$x = 0$. Using an appropriate piecewise uniform mesh and a standard finite difference operator, Shishkin⁷ establishes a first order parameter-uniform⁶ numerical method for this transport problem.

In the context of two-parameter singularly perturbed elliptic problems,^{8, §3 and Remark 8.3} first-order problems of the form

$$\mu \vec{a} \cdot \nabla u - bu = f(x, y), \quad (x, y) \in [0, 1]^2, \quad u(x, 0), u(0, y) \text{ given}$$

were examined. Boundary layers of order $O(\mu)$ appear near the edges $x = 0, y = 0$. (If $u(x, 1), u(1, y)$ are given instead of $u(x, 0), u(0, y)$, the layers will form along $x = 1$ and $y = 1$.) Using an appropriate Shishkin mesh,⁸ a parameter-uniform error bound of the form ($N^{-1} \ln N$) can be established.

In this paper, we examine linear singularly perturbed transport problems of the form

$$u_t + au_x + bu = f(x, t; \varepsilon); \quad u(0, t) = \psi(t; \varepsilon); \quad u(x, 0) = \phi(x; \varepsilon), \quad (1)$$

where layers (boundary and/or interior) are generated by the fact that layers are present in one or more of the functions ψ, ϕ, f . In contrast to the problems examined in Shishkin⁷ and O'Riordan and Pickett,⁸ the characteristic curves associated with (1) do not depend on the singular perturbation parameter. Moreover, under the assumption $a(x, t) \geq \alpha > 0, \forall (x, t)$, the tangents to the characteristic curves always have a finite slope.

The construction of an appropriate piecewise-uniform Shishkin mesh is the central component in our numerical methods. This construction relies on the existence of a priori information about the location and width⁶ of all boundary or interior layers within the solution. This a priori information can sometimes be derived from asymptotic analysis. In the case of this paper, this information is deduced from the bounds in (7), (16) and (21) on the derivatives of the problem data. In the case of non-linear problems, this asymptotic information can be more difficult to identify; but for particular non-linear problems (e.g., O' Riordan and Quinn^{9,10}), this information is available. However, although sufficient a priori information may exist for a certain class of singularly perturbed problems, the proof of parameter-uniform convergence of the numerical approximations may be difficult to complete, especially in the case of non-linear problems. In this paper, we supply proofs of uniform convergence for the three linear problem classes considered.

The paper is structured as follows. In Section 2, a comparison principle is given and the regularity of the solution is discussed for non-singularly perturbed transport problems. A result of convergence for a classical scheme is established when the solution u of problem (1) satisfies $u \in C^1(\bar{\Omega})$. In Sections 3–5, three problem classes of singularly perturbed problems are considered. The boundary or interior layers are generated due to the forcing term, the initial or boundary conditions depending on the singular perturbation parameter. The interior layers are located along the characteristic curves associated with problem (1) and the numerical methods will need to align the mesh to this characteristic curve in order to accurately track the interior layer,¹¹ which are described in Section 4 and Appendix A.1. We construct and analyse parameter-uniform numerical methods for all the singularly perturbed transport problems considered of the form given in (1). In Section 6, we examine a problem motivated by a mathematical model of fluid–particle interaction in particle-laden flows⁵; the solution is decomposed into several components which are approximated using the algorithms described in the three previous sections. The numerical results indicate that our method generates almost first-order global approximations to the solution of this model. Finally, we draw some conclusions.

Notation: Throughout the paper, C denotes a generic constant that is independent of the singular perturbation parameter ε and all the discretization parameters. The L_∞ norm on a domain D will be denoted by $\|\cdot\|_D$. If the norm is not subscripted, then $\|\cdot\| = \|\cdot\|_{\bar{\Omega}}$.

2 | NON-SINGULARLY PERTURBED PROBLEM

Consider first-order differential operators of the form

$$L\omega := \omega_t + a(x, t)\omega_x + b(x, t)\omega,$$

and the domain $\Omega := (0, L] \times (0, T]$.

Lemma 1. *Assume $\omega(x, 0) \geq 0, 0 \leq x \leq L, a(x, t) \geq 0, (x, t) \in \bar{\Omega}, a, b \in C^0(\bar{\Omega})$ and $\omega \in C^1(\Omega) \cap C^0(\bar{\Omega})$. If $\omega(0, t) \geq 0$ or $\omega_x(0^+, t) < 0$ for $t \in (0, T]$ and $L\omega \geq 0$ in Ω , then $\omega(x, t) \geq 0, \forall (x, t) \in \bar{\Omega}$.*

Proof. The proof is by contradiction. Assume $\omega < 0$ within $\bar{\Omega}$. Let $v(x, t) = \omega(x, t)e^{-\beta t}, \beta > \|b\|$ and $v(p, q) := \min_{\bar{\Omega}} v(x, t) < 0$. By our assumptions, $q \neq 0, p \neq 0$. Hence $(p, q) \in \Omega$ where $v_x(p^-, q) \leq 0, v_t(p, q^-) \leq 0$. However, then

$$L\omega(p, q) = e^{\beta q}(v_t + av_x + (b + \beta)v)(p, q) < 0,$$

which is a contradiction. \square

Consider the initial-boundary value problem: Find u such that

$$Lu = f(x, t), (x, t) \in \Omega, u(0, t) = \psi(t), u(x, 0) = \phi(x); \quad (2a)$$

$$a(x, t) \geq \alpha > 0, b(x, t) \geq 0, (x, t) \in \bar{\Omega}; \quad (2b)$$

$$\psi \in C^2([0, T]), \phi \in C^2([0, L]), a, b, f \in C^2(\bar{\Omega}). \quad (2c)$$

There is no loss in generality in assuming that $b \geq 0$, as we simply use the transformation $u^T = ue^{-\beta t}, \beta > \|b\|$ and solve $Lu^T + \beta u^T = e^{\beta t}f$ for u^T . From Bobisud,¹² Appendix in order for $u \in C^2(\bar{\Omega})$, we require the following compatibility conditions on the data:

$$\phi(0) = \psi(0); \quad (3a)$$

$$\psi'(0) + a(0, 0)\phi'(0) + b(0, 0)\psi(0) = f(0, 0); \quad (3b)$$

$$\begin{aligned} & [f_t(0, 0) - b_t(0, 0)\psi(0) - b(0, 0)\psi'(0) - \psi''(0)] \\ & + \phi'(0) [a(0, 0)(b(0, 0) + a_x(0, 0)) - a_t(0, 0)] + a^2(0, 0)\phi''(0) \\ & = a(0, 0) [f_x(0, 0) - b_x(0, 0)\psi(0)]. \end{aligned} \quad (3c)$$

As in Bobisud,¹² define the characteristic curve passing through the point (s, τ) by $x = g(t; s, \tau)$, where $x = g(t)$ is the solution of the initial value problem

$$\frac{dx}{dt} = a(x, t), \quad x(\tau) = s.$$

Define $\Gamma(s, \tau)$ such that $g(\Gamma(s, \tau); s, \tau) = 0$. The point $(x, t) = (0, \Gamma(s, \tau))$ is where the characteristic curve through the point (s, τ) intercepts the axis $x = 0$. Define the two subregions $D_1 := \{(x, t) | x > g(t; 0, 0)\}, D_2 := \{(x, t) | x < g(t; 0, 0)\}$. The exact solution of problem (2) is then given by¹²

$$\begin{aligned} u(s, \tau) &= \phi(g(0; s, \tau))B(0, \tau; s, \tau) + \\ &+ \int_{z=0}^{\tau} f(g(z; s, \tau), z)B(\tau, z; s, \tau)dz, \quad (s, \tau) \in D_1; \end{aligned} \quad (4a)$$

$$\begin{aligned} u(s, \tau) &= \psi(\Gamma(s, \tau))B(\Gamma(s, \tau), \tau; s, \tau) + \\ &+ \int_{z=\Gamma(s, \tau)}^{\tau} f(g(z; s, \tau), z)B(\tau, z; s, \tau)dz, \quad (s, \tau) \in D_2; \end{aligned} \quad (4b)$$

where

$$B(\eta, \iota; s, \tau) := e^{-\int_{t=\eta}^{\iota} b(g(t; s, \tau), t)dt}.$$

If (3a) is not satisfied, then the solution of problem (2) is discontinuous across the characteristic curve $x = g(t; 0, 0)$. If (3b) is not satisfied, then the solution u of problem (2), (3a) is such that $u \in C^0(\bar{\Omega}) \setminus C^1(\bar{\Omega})$. Finally, if (3c) is not satisfied, then the solution u of problem (2), (3a), (3b) is such that $u \in C^1(\bar{\Omega}) \setminus C^2(\bar{\Omega})$. We associate the following four functions $\{\chi_i\}_{i=0}^3$, with the compatibility conditions (3):

$$L\chi_0(x, t) = 0, \quad L\chi_1(x, t) = 1, \quad (x, t) \in \Omega, \quad (5a)$$

$$L\chi_2(x, t) = x, \quad L\chi_3(x, t) = t, \quad (x, t) \in \Omega, \quad (5b)$$

$$\chi_0(0, t) = 0, \quad t > 0, \quad \chi_0(x, 0) = 1, \quad x \geq 0, \quad (5c)$$

$$\chi_i(0, t) = 0, \quad t > 0, \quad \chi_i(x, 0) = 0, \quad x \geq 0, \quad i = 1, 2, 3; \quad (5d)$$

where $\chi_0 \notin C^0(\bar{\Omega})$, $\chi_1 \in C^0(\bar{\Omega}) \setminus C^1(\bar{\Omega})$ and $\chi_2, \chi_3 \in C^1(\bar{\Omega}) \setminus C^2(\bar{\Omega})$. Explicit representations for χ_0 and χ_1 can be determined using (4). In general, for the solution u of problem (2), we note that

$$\begin{aligned} u(x, t) - (\psi(0) + (\phi(0) - \psi(0))\chi_0(x, t)) &\in C^0(\bar{\Omega}) \setminus C^1(\bar{\Omega}); \\ u(x, t) - (\psi(0) + (\phi(0) - \psi(0))\chi_0(x, t)) - A\chi_1(x, t) &\in C^1(\bar{\Omega}) \setminus C^2(\bar{\Omega}); \\ \text{where } A &:= f(0, 0) - (\psi'(0) + a(0, 0)\phi'(0) + b(0, 0)\psi(0)). \end{aligned}$$

After separating off the singular terms χ_0 and χ_1 , we can use a simple numerical method to generate an approximation to the solution of a problem of the form (2), (3a), (3b). Select a set of mesh points

$$\bar{\Omega}^{N,M} := \{(x_i, t_j) | x_0 = 0, t_0 = 0, x_N = L, t_M = T\}_{i,j=0}^{N,M},$$

where the mesh steps are denoted by $h_i := x_i - x_{i-1}$, $1 \leq i \leq N$; $k_j := t_j - t_{j-1}$, $1 \leq j \leq M$ and $\max_i h_i \leq CN^{-1}$, $\max_j k_j \leq CM^{-1}$. Define the set of interior mesh points as $\Omega^{N,M} := \{(x_i, t_j)\}_{i,j=1}^{N,M}$. We can discretize problem (2) using an upwinded finite difference operator¹ of the form:

$$L^{N,M}U(x_i, t_j) = f(x_i, t_j), \quad (x_i, t_j) \in \Omega^{N,M}, \quad (6a)$$

$$U(0, t_j) = u(0, t_j), \quad t_j > 0, \quad U(x_i, 0) = u(x_i, 0), \quad x_i \geq 0; \quad (6b)$$

$$\text{where } L^{N,M}U(x_i, t_j) := (D_t^- + a(x_i, t_j)D_x^- + b(x_i, t_j)I)U(x_i, t_j). \quad (6c)$$

Similarly to the continuous problem, the discrete operator $L^{N,M}$ satisfies a discrete comparison principle.

We form a global approximation \bar{U} to the solution of (2), (3a), using

$$\bar{U}(x, t) := \sum_{i=0, j=1}^{N,M} U(x_i, t_j) \varphi_i(x) \eta_j(t),$$

where $\varphi_i(x)$ is the standard hat function centred at $x = x_i$ and $\eta_j(t) := (t - t_{j-1})/k_j$, $t \in [t_{j-1}, t_j]$, $\eta_j(t) := 0$, $t \notin [t_{j-1}, t_j]$.

Theorem 1. *If U is the solution of (6) and $u \in C^1(\bar{\Omega})$ is the solution of (2), then*

$$\|\bar{U} - u\| \leq C(N^{-1} + M^{-1}).$$

Proof. As $\frac{dx}{dt} > 0$, then at each time level $t = t_*$, there is only one point (x_*, t_*) where the characteristic curve $x = g(t; 0, 0)$ cuts the line $t = t_*$. From the explicit expression in (4), we see that the second-order derivatives of χ_2 and χ_3 are continuous at all points except for the points on the curve $x = g(t_*; 0, 0)$. Moreover, the second derivatives are bounded along this characteristic curve $Y = \{(x_*, t_*) = (g(t_*; 0, 0), t_*), 0 \leq t_* \leq T\}$. That is,

$$|u_{xx}(x_*^\pm, t_*)| \leq C, \quad \|u_{xx}\|_{\Omega \setminus Y} \leq C, \quad |u_{tt}(x_*, t_*^\pm)| \leq C, \quad \|u_{tt}\|_{\Omega \setminus Y} \leq C.$$

¹We use the following notation for the finite difference operators:

$$D_t^- Y(x_i, t_j) := \frac{Y(x_i, t_j) - Y(x_i, t_{j-1})}{k_j}, \quad D_x^- Y(x_i, t_j) := \frac{Y(x_i, t_j) - Y(x_{i-1}, t_j)}{h_i}.$$

For each $t = t_j$, there exists a unique subinterval $[x_{I-1}, x_I]$ such that $x_*^I \in (x_{I-1}, x_I)$ and $x_*^I = g(t_j)$. For this particular interval,

$$\begin{aligned} \left(\frac{\partial}{\partial x} - D_x^- \right) u(x_i, t_j) &= \frac{1}{h_i} \int_{s=x_{I-1}}^{x_i} u_x(x_i, t_j) - u_x(s, t_j) ds \\ &= \frac{1}{h_i} \int_{s=x_{I-1}}^{x_i} \left(\int_{r=s}^{x_*^I} u_{xx}(r, t_j) dr + \int_{r=x_*^I}^{x_i} u_{xx}(r, t_j) dr \right) ds. \end{aligned}$$

In an analogous fashion, for each $x = x_i$, there exists a unique subinterval $[t_{J-1}, t_J]$ such that $t_*^J \in (t_{J-1}, t_J)$ and $x_i = g(t_*^J)$. For this particular interval,

$$\left(\frac{\partial}{\partial t} - D_t^- \right) u(x_i, t_j) = \frac{1}{k_j} \int_{s=t_{J-1}}^{t_j} \left(\int_{r=s}^{t_*^J} u_{tt}(x_i, r) dr + \int_{r=t_*^J}^{t_j} u_{tt}(x_i, r) dr \right) ds.$$

Hence, inside of these intervals, we have

$$\left| \left(\frac{\partial}{\partial x} - D_x^- \right) u(x_i, t_j) \right| \leq CN^{-1}, \quad \left| \left(\frac{\partial}{\partial t} - D_t^- \right) u(x_i, t_j) \right| \leq CM^{-1}.$$

On the other hand, truncation error estimates outside of these particular subintervals can be easily obtained using that u_{xx} and u_{tt} are continuous functions. Therefore, we have

$$|L^{N,M}(u - U)(x_i, t_j)| \leq CN^{-1} + CM^{-1}, \quad (x_i, t_j) \in \Omega^{N,M}.$$

As the upwind operator $L^{N,M}$ satisfies a discrete comparison principle, it follows that

$$|(u - U)(x_i, t_j)| \leq CN^{-1} + CM^{-1}.$$

This nodal error bound extends to a global error bound using standard interpolation error estimates. \square

Remark 1. If instead of separating away the term involving $\chi_1(x, t)$, one could use the numerical method to generate an approximation, when $u \in C^0(\bar{\Omega}) \setminus C^1(\bar{\Omega})$. In this case, unlike Theorem 2, the computed order of convergence in our numerical experiments reduce to 0.5.

In the remaining sections, we construct numerical methods in the case where the problem (2) is singularly perturbed.

3 | FLOW TOWARDS AN ATTRACTIVE FORCE

In the first problem class to be examined in this paper, the forcing term has a layer at the outflow ($x = L$) of the domain. Consider problem (2), (3) with the additional conditions

$$\left| \frac{\partial^{i+j}}{\partial x^i \partial t^j} f(x, t; \epsilon) \right| \leq \frac{C_1}{\epsilon^{1+i}} e^{\frac{x-L}{\epsilon}}; \quad 0 \leq i + j \leq 2, \quad (7a)$$

$$\frac{\partial^{i+j} f}{\partial x^i \partial t^j}(0, 0) = 0, \quad 0 \leq i + j \leq 1. \quad (7b)$$

Then, the solution u can be decomposed into the sum of a regular component $v \in C^2(\bar{\Omega})$ and a layer component $w \in C^2(\bar{\Omega})$ defined by

$$Lv = 0, \quad (x, t) \in \Omega; \quad v = u, \quad (x, t) \in \partial\Omega := \bar{\Omega} \setminus \Omega; \quad (8a)$$

$$Lw = f, \quad (x, t) \in \Omega; \quad w = 0, \quad (x, t) \in \partial\Omega. \quad (8b)$$

In this section, the problem data a, b, ψ, ϕ , are smooth functions that do not depend on the singular perturbation parameter ε . By Lemma 1,

$$|u(x, t)| \leq \|\phi\|_{[0, T]} + \|\psi\|_{[0, L]} + \frac{C_1}{\alpha} e^{\frac{x-L}{\varepsilon}}.$$

Lemma 2. For all $(x, t) \in \bar{\Omega}$, the components in (8) satisfy

$$\left\| \frac{\partial^{i+j} v}{\partial x^i \partial t^j} \right\| \leq C, \quad 0 \leq i + j \leq 2; \quad (9a)$$

$$|w(x, t)| \leq C e^{\frac{x-L}{\varepsilon}} \left(1 - e^{-\frac{\|a\|t}{\varepsilon}} \right); \quad (9b)$$

$$\left| \frac{\partial^{i+j} w(x, t)}{\partial x^i \partial t^j} \right| \leq C \varepsilon^{-(i+j)} e^{\frac{x-L}{\varepsilon}}, \quad 1 \leq i + j \leq 2. \quad (9c)$$

Proof. As the data for the problem (8a) are independent of the parameter ε and since $v \in C^2(\bar{\Omega})$, the bounds on the derivatives of v follow immediately.

Using Lemma 1 with the obvious barrier function yields the bound on $w(x, t)$. Since $w_x \in C^1(\bar{\Omega})$, it satisfies the first-order problem

$$Lw_x + a_x w_x = f_x - b_x w, \quad w_x(x, 0) = 0, \quad w_x(0, t) = \frac{f(0, t)}{a(0, t)}. \quad (10)$$

Using $w_1 := e^{-\kappa t} w_x$, $\kappa := \min\{b + a_x, 0\}$ and Lemma 1 again, we establish the bound

$$|w_x(x, t)| \leq C \varepsilon^{-1} e^{\frac{x-L}{\varepsilon}} \text{ and then } |w_t(x, t)| \leq C \varepsilon^{-1} e^{\frac{x-L}{\varepsilon}}.$$

Using (4) a closed form representation of the solution of (10) exists. Differentiating this expression (w.r.t. x) and using $g(z; x, t) \leq \|a\|(z - t) + x$, we have that

$$\left| \frac{\partial^2 w}{\partial x^2}(x, t) \right| \leq C \begin{cases} \int_{s=0}^t \varepsilon^{-3} e^{\frac{\|a\|(s-t)+x-L}{\varepsilon}} ds, & (x, t) \in D_1, \\ \left(\int_{s=0}^t + \int_{s=0}^{\Gamma(x, t)} \right) \left| \frac{\partial(f_x - b_x w)(g(s; x, t), t)}{\partial x} \right| ds, & (x, t) \in D_2. \end{cases}$$

Hence

$$\left| \frac{\partial^2 w}{\partial x^2}(x, t) \right| \leq C \varepsilon^{-2} e^{\frac{x-L}{\varepsilon}}.$$

Use the differential equation $u_{tx} = (f - bu - au_x)_x$ to derive bounds on u_{tx} and $u_{tt} = (f - bu - au_x)_t$ to derive bounds on u_{tt} . \square

The layer function can be further decomposed into

$$w(x, t) = w_0(x, t) + w_1(x, t), \quad \text{where} \quad (11a)$$

$$Lw_0 = 0, \quad (x, t) \in \Omega, \quad w_0(0, t) = 0, \quad w_0(x, 0) = \omega(x), \quad (11b)$$

$$a(x, 0) \frac{d\omega}{dx} + b(x, 0)\omega = f(x, 0), \quad 0 < x \leq L, \quad \omega(0) = 0. \quad (11c)$$

Observe that, for $0 < p < 1$,

$$\begin{aligned} \left| \frac{d^i \omega(x)}{dx^i} \right| &\leq C \varepsilon^{-i} e^{\frac{x-L}{\varepsilon}} i = 0, 1, 2; \left| \frac{\partial^j}{\partial t^j} w_0(x, t) \right| \leq C \varepsilon^{-j} e^{\frac{x-L}{\varepsilon}} e^{-\frac{pat}{\varepsilon}}, j = 0, 1, \\ L \left(\frac{\partial w_1}{\partial t} \right) &= f - a_t \frac{\partial w_1}{\partial x} - b_t w_1, \quad \frac{\partial w_1}{\partial t}(0, t) = \frac{\partial w_1}{\partial t}(x, 0) = 0. \end{aligned}$$

Using the arguments in the previous Lemma 2, we can establish that

$$\left| \frac{\partial^j w_1(x, t)}{\partial t^j} \right| \leq C \varepsilon^{1-j} e^{\frac{x-L}{\varepsilon}}, \quad j = 1, 2. \quad (12)$$

To capture the layer near $x = L$, we define a piecewise-uniform Shishkin mesh⁶ in both space and time, which we denote by $\bar{\Omega}_S^N$. The space domain is split by $[0, L] = [0, L - \sigma] \cup [L - \sigma, L]$ and the time domain is subdivided into $[0, T] = [0, \tau] \cup [\tau, T]$. In each coordinate direction, half of the mesh points are uniformly distributed in each subinterval. The transition points are defined to be

$$\sigma := \min \left\{ \frac{L}{2}, \varepsilon \ln N \right\} \text{ and } \tau := \min \left\{ \frac{T}{2}, C_2 \varepsilon \ln M \right\}, \quad C_2 > \alpha^{-1}.$$

The two mesh steps in space and time are denoted by

$$H = 2 \frac{L - \sigma}{N}, \quad h = 2 \frac{\sigma}{N}, \quad K = 2 \frac{T - \tau}{M}, \quad k = 2 \frac{\tau}{M}.$$

On this piecewise-uniform mesh, we use a classical upwinded finite difference operator at all points except at the transition point where $x_i = L - \sigma$. The discrete problem is: Find U such that

$$L_F^{N,M} U(x_i, t_j) = f(x_i, t_j), \quad (x_i, t_j) \in \Omega_S^N; \quad (13a)$$

$$U(0, t_j) = u(0, t_j), \quad t_j \geq 0, \quad U(x_i, 0) = u(x_i, 0), \quad 0 \leq x_i \leq L, \quad (13b)$$

where the fitted finite difference operator $L_F^{N,M}$ is defined as

$$L_F^{N,M} U(x_i, t_j) := \begin{cases} L^{N,M} U(x_i, t_j), & \text{if } x_i \neq L - \sigma, \\ \left(L^{N,M} + a(x_i, t_j) \left(\frac{\rho}{1-e^{-\rho}} - 1 \right) D_x^- \right) U(x_i, t_j), & \text{if } x_i = L - \sigma, \end{cases} \quad (13c)$$

with $\rho := H/\varepsilon$. A standard proof-by-contradiction argument can be used to establish the next result.

Lemma 3. *Let $S = (p_1, p_2] \times (q_1, q_2]$ be a subdomain of Ω . For any mesh function Z , if $Z(x_i, q_1) \geq 0$, $p_1 \leq x_i \leq p_2$, $Z(p_1, t_j) \geq 0$, $q_1 \leq t_j \leq q_2$ and $L_F^{N,M} Z(x_i, t_j) \geq 0$, $(x_i, t_j) \in S$, then $Z(x_i, t_j) \geq 0$, $(x_i, t_j) \in \bar{S}$.*

The discrete solution can be decomposed into a regular and singular component, $U = V + W$, where the regular component satisfies

$$\begin{aligned} L_F^{N,M} V(x_i, t_j) &= 0, \quad (x_i, t_j) \in \Omega_S^N, \\ V(0, t_j) &= u(0, t_j), \quad t_j \geq 0, \quad V(x_i, 0) = u(x_i, 0), \quad 0 \leq x_i \leq L, \end{aligned}$$

and the layer function satisfies

$$\begin{aligned} L_F^{N,M} W(x_i, t_j) &= f(x_i, t_j), \quad (x_i, t_j) \in \Omega_S^N, \\ W(0, t_j) &= 0, \quad t_j \geq 0, \quad W(x_i, 0) = 0, \quad 0 \leq x_i \leq L. \end{aligned}$$

Lemma 4. *The discrete boundary layer component satisfies*

$$|W(x_i, t_j)| \leq CN^{-1}, \quad x_i \leq L - \sigma, \quad t_j \geq 0.$$

Proof. For all $x_i < L - \sigma$, consider the barrier function

$$B_1(x_i, t_j) := \frac{C_1}{\varepsilon} \frac{H}{\alpha} \sum_{n=1}^i e^{\frac{x_n-L}{\varepsilon}} \text{ with } D_x^- B_1(x_i, t_j) = \frac{C_1}{\alpha \varepsilon} e^{\frac{x_i-L}{\varepsilon}},$$

and the constant C_1 is given in (7). From Lemma 3, at all mesh points $x_i < L - \sigma$, outside the layer

$$L_F^{N,M} B_1(x_i, t_j) \geq a(x_i, t_j) D_x^- B_1(x_i, t_j) \geq |f(x_i, t_j)|.$$

Hence, for $x_i < L - \sigma$,

$$W(x_i, t_j) \leq B_1(x_i, t_j) \leq C \frac{H}{\varepsilon} e^{\frac{x_i-L}{\varepsilon}} \frac{1 - e^{-\frac{L}{\varepsilon}}}{1 - e^{-\frac{H}{\varepsilon}}} \leq C e^{\frac{x_{i+1}-L}{\varepsilon}} \leq C e^{-\frac{\sigma}{\varepsilon}} \leq CN^{-1}.$$

At the transition point $x_i = L - \sigma$, use Lemma 3 and the barrier function

$$B_2(L - \sigma, t_j) = C_1 \frac{H}{\varepsilon} e^{-\frac{\sigma}{\varepsilon}} \frac{(1 - e^{-\rho})}{\rho} + CN^{-1}, \quad B_2(L - \sigma - H, t_j) = CN^{-1},$$

to complete the proof. \square

Theorem 2. *If U is the solution of (13) and u is the solution of (2), (3), (7), then*

$$\|\bar{U} - u\| \leq C(N^{-1} \ln N + M^{-1} \ln M).$$

Proof. The nodal error is decomposed into two components

$$u - U = (v - V) + (w - W).$$

As the derivatives of v are bounded independently of ε , we have the truncation error bounds

$$\begin{aligned} |L_F^{N,M}(V - v)(x_i, t_j)| &\leq C(N^{-1} + M^{-1}), \quad x_i \neq L - \sigma \\ |L_F^{N,M}(V - v)(L - \sigma, t_j)| &\leq C(N^{-1} + M^{-1}) + C \frac{\rho}{1 - e^{-\rho}}. \end{aligned}$$

Use the discrete barrier function

$$B_3(x_i, t_j) = CM^{-1}t_j + CN^{-1} \begin{cases} x_i, & x_i < L - \sigma, \\ x_i + 1, & x_i \geq L - \sigma, \end{cases}$$

and the discrete comparison principle (Lemma 3) to deduce the nodal error bound

$$|(V - v)(x_i, t_j)| \leq B_3(x_i, t_j) \leq C(N^{-1} + M^{-1}). \tag{14}$$

Outside the fine mesh, using (9b) and Lemma 4, we have that

$$|(W - w)(x_i, t_j)| \leq |W(x_i, t_j)| + |w(x_i, t_j)| \leq CN^{-1}, \quad x_i \leq L - \sigma.$$

Within the fine mesh in both space and time, we have the truncation error bound for $L - \sigma < x_i < L, t_j \leq \tau$,

$$|L_F^{N,M}(W - w)(x_i, t_j)| \leq C \frac{N^{-1} \ln N + M^{-1} \ln M}{\varepsilon} e^{\frac{x_i-L}{\varepsilon}},$$

where we use $\varepsilon^{-1} \leq C_2 \ln N$ in the case where the mesh is piecewise uniform in space. For $L - \sigma < x_i < L, \tau < t_j \leq T$, using (11) and (12)

$$\left| \left(D_t^- - \frac{\partial}{\partial t} \right) w \right| \leq C \varepsilon^{-1} e^{-\frac{p\alpha\tau}{\varepsilon}} e^{\frac{x_i-L}{\varepsilon}} + \left| \left(D_t^- - \frac{\partial}{\partial t} \right) w_1 \right| \leq C \frac{M^{-1}}{\varepsilon} e^{\frac{x_i-L}{\varepsilon}}.$$

Hence, for $L - \sigma < x_i < L, t_j > 0$,

$$|L_F^{N,M}(W - w)(x_i, t_j)| \leq C \frac{N^{-1} \ln N + M^{-1} \ln M}{\varepsilon} e^{\frac{x_i-L}{\varepsilon}},$$

and $|(W - w)(L - \sigma, t_j)| \leq CN^{-1}, (W - w)(x_i, 0) = 0$. Then, using

$$B_4(x_i, t_j) = C(N^{-1} \ln N + M^{-1} \ln M) e^{\frac{x_i-L}{\varepsilon}},$$

as a discrete barrier function in the fine mesh, we can establish for sufficiently large N and M that

$$|(W - w)(x_i, t_j)| \leq C(N^{-1} \ln N + M^{-1} \ln M) e^{\frac{x_i-L}{\varepsilon}}; \quad (15)$$

where we use the fact that for $0 < z \leq \delta$

$$\frac{1 - e^{-z}}{z} \geq \frac{1 - e^{-\delta}}{\delta} \geq \frac{1}{2} \text{ for sufficiently small } \delta.$$

Combining all of the bounds (14) and (15), we deduce the nodal error bound

$$\|u - U\|_{\Omega_S^N} \leq C(N^{-1} \ln N + M^{-1} \ln M).$$

Combine the arguments in Farrell et al.⁶, Theorem 3.12 with the interpolation bounds in Stynes and O'Riordan¹³, Lemma 4.1 and the bounds on the derivatives of the components v, w to extend this bound to a global error bound. \square

Remark 2. If, in addition to the constraints (7), we have $f(x, 0) = 0, x \in [0, L]$, then $w_0 \equiv 0$ in (11) and the bounds in (12) apply to w . Hence, in this case, one can use a uniform mesh in time and retain the same error bound given in Theorem 2.

4 | TRANSPORTING A PULSE

In the second problem class, the initial or boundary condition contains a layer, which generates an interior layer in the solution of the transport equation. Consider problem (2), (3) with an ε -dependent initial condition

$$u(x, 0) = \phi_1(x) + \phi_2(x; \varepsilon), \quad (16a)$$

where $\phi_1(x)$ is a smooth function and ϕ_2 has a layer in an interior point d with $0 < d < L$ in that

$$\phi_2^{(i)}(0) = 0, |\phi_2^{(i)}(x)| \leq C \varepsilon^{-i} e^{-\frac{|x-d|}{\varepsilon}}, 0 \leq i \leq 2; \quad (16b)$$

or if the layer occurs at the endpoint $d = 0$ then

$$|\phi_2^{(i)}(x)| \leq C x^\ell \varepsilon^{-(\ell+i)} e^{-\frac{x}{\varepsilon}}, 0 \leq i \leq 2; \ell \geq 3. \quad (16c)$$

The condition on ℓ is required to guarantee the regularity of the singular component (18) associated with u . In this section, the problem data, a, b, f , are smooth functions that do not depend on the singular perturbation parameter ε . The pulse in the initial condition is transported along the characteristic curve $x = g(t; d, 0)$, which is the solution of the initial value problem

$$\frac{dx}{dt} = a(x, t), \quad x(0) = d. \quad (17)$$

Note that

$$\begin{aligned} |\phi_2(x)| &\leq CN^{-1}, & \text{if } |x - d| \geq \varepsilon \ln N \text{ and } d > 0 \\ |\phi_2(x)| &\leq C_q N^{-(q-\ell)} (N^{-1} \ln N)^\ell, & \text{if } x \geq q\varepsilon \ln N \text{ and } d = 0. \end{aligned}$$

If $\varepsilon \ln N$ is sufficiently large ($\geq L/2$), then we can solve for u using a classical scheme on a uniform mesh. Otherwise, we align the mesh along the characteristic curve passing through $(d, 0)$.

The solution u can be decomposed into the sum of a regular component $v \in C^2(\bar{\Omega})$ and a layer component $w \in C^2(\bar{\Omega})$, defined as the solutions of

$$Lv = f, \quad (x, t) \in \Omega; \quad v(0, t) = u(0, t), \quad v(x, 0) = \phi_1(x), \quad (18a)$$

$$Lw = 0, \quad (x, t) \in \Omega; \quad w(0, t) = 0, \quad w(x, 0) = \phi_2(x, \varepsilon). \quad (18b)$$

Based on this decomposition, we first generate a discrete approximation V to v using a uniform rectangular mesh and simple upwinding. Consider the transformed variables, $\tilde{u}(s, t) = u(x, t)$ where $s := x - g(t; d, 0)$ and $g'(t; d, 0) = a(g(t; d, 0), t)$, then

$$\tilde{w}_t + [\tilde{a}(s, t) - \tilde{a}(0, t)] \tilde{w}_s + \tilde{b}\tilde{w} = 0, \quad \tilde{w}(s, 0) = \phi_2(s + d).$$

Note that

$$\left| \frac{\partial^{i+j} \tilde{w}}{\partial s^i \partial t^j}(s, t) \right| \leq C\varepsilon^{-i} e^{-\frac{|s|}{\varepsilon}}, \quad 0 \leq i + j \leq 2.$$

Throughout the paper, we assume that the characteristic curves $x = g(t; d, 0)$ can be explicitly determined. To generate a parameter-uniform approximation to w , we solve the problem in the transformed variables (s, t) . We describe below a numerical scheme where it is assumed that a_x does not change sign either side of $x = g(t; d, 0)$. Otherwise, a more general scheme is required which is described in Appendix A.1 of this paper.

We use a uniform mesh in time and a piecewise-uniform mesh in space, where the space domain is split into the subdomains

$$\begin{aligned} [-d, -\sigma_d] \cup [-\sigma_d, \sigma_d] \cup [\sigma_d, L-d], \\ \sigma_d := \min \left\{ \frac{d}{2}, \frac{L-d}{2}, \varepsilon \ln N \right\}, \quad \text{if } d > 0, \end{aligned} \quad (19a)$$

$$[0, \sigma_0] \cup [\sigma_0, L], \quad \sigma_0 := \min \left\{ \frac{L}{2}, (\ell+1)\varepsilon \ln N \right\}, \quad \text{if } d = 0. \quad (19b)$$

Then, consider the following upwind scheme² on the subdomain $\tilde{\Omega} := (-d, L-d) \times (0, T]$

$$D_t^- \tilde{W} + [\tilde{a}(s_i, t_j) - \tilde{a}(0, t_j)] D_s^* \tilde{W} + \tilde{b}\tilde{W} = 0, \quad (s_i, t_j) \in \tilde{\Omega}; \quad (20a)$$

$$\tilde{W}(-d, t_j) = \tilde{W}(L-d, t_j) = 0; \quad \tilde{W}(s_i, 0) = \phi_2(s_i + d). \quad (20b)$$

²The upwind finite difference operator is defined to be

$$b(s_i, t_j) D_s^* \tilde{W} := 0.5 ((b(s_i, t_j) + |b(s_i, t_j)|) D_s^- + (b(s_i, t_j) - |b(s_i, t_j)|) D_s^+) \tilde{W}.$$

At $s_i = 0$, the stencil collapses to the two point scheme

$$\left(D_t^- \widetilde{W} + \widetilde{b} \widetilde{W} \right) (0, t_j) = 0, \quad t_j > 0, \quad \widetilde{W}(0, 0) = \phi_2(d). \quad (20c)$$

Hence, $\widetilde{W}(0, t_j)$ can be easily determined and the remaining nodal values for the interior layer function, $\widetilde{W}(s_i, t_j), s_i \in (-d, L - d) \setminus \{0\}$, can be determined separately on either side of $s = 0$. The layer component w is similarly approximated when $d = 0$.

We can generate a global approximation \bar{W} to w over the region $\bar{\Omega}^3$ using bilinear interpolation. Then, set

$$\bar{W} \equiv 0 \text{ on } \bar{\Omega} \setminus \{(x, t), -d + g(t; d, 0) \leq x \leq L, 0 \leq t \leq T\}.$$

We form $\bar{U} = \bar{V} + \bar{W}$, where \bar{V} is the global approximation to v with a classical scheme on a uniform mesh, and we can deduce the global error bound, over $\bar{\Omega}$,

$$\|u - \bar{U}\| \leq CN^{-1}(\ln N)^2 + CM^{-1}$$

for the problem class (2), (3), (16).

A related problem to (2), (3), (16) when the pulse occurs in the boundary condition is considered in Appendix A.1. The numerical approximation to this problem class is used in Section 6.

Remark 3. The construction of the numerical schemes of this section and Appendix A.1 is based on the characteristic curves $g(t; d, 0)$. If the location of the characteristic curves need to be estimated, then we can use a Runge–Kutta method to solve the non-linear ode $x'(t) = a(x, t), x(0) = s$. However, to preserve parameter-uniform convergence then for any characteristic curves passing through $(x(0), 0)$ where $x(0) \in [d - 2\sigma_d, d + 2\sigma_d]$ needs to be determined so that $|x(t_i) - x^N(t_i)| \leq \sigma_d$ for an approximate curve $(x^N(t), t)$.

5 | FLOW AWAY FROM AN ATTRACTIVE FORCE

In the third problem class to be examined, the forcing term has a layer at the inflow of the domain. This generates a boundary layer on the left and an interior layer emanating from the initial inflow boundary point.

Consider problem (2), (3) with the additional conditions

$$a_t(0, 0) = 0, \quad \left| \frac{\partial^{i+j} f}{\partial x^i \partial t^j} (x, t) \right| \leq C x^{2-i} \varepsilon^{i-3} e^{-\frac{x}{\varepsilon}}, \quad 0 \leq i + j \leq 2; \quad (21a)$$

$$a \in C^3(\bar{\Omega}), \quad b(x, t) \equiv 0, \quad f(x, t) = f(x), \quad \forall (x, t) \in \bar{\Omega}. \quad (21b)$$

In this section, the problem data, a, b, ψ, ϕ , are smooth functions that do not depend on the singular perturbation parameter ε . By Lemma 1,

$$|u(x, t)| \leq \frac{C}{\alpha} \left(1 - e^{-\frac{x}{\varepsilon}} \right).$$

Notation: For each $t \geq 0$, define $w_0, w_1 \in C^2(\bar{\Omega})$ as the solutions of

$$a(x, t) \frac{\partial w_0}{\partial x} = f(x), \quad w_0(\infty, t) = 0, \quad (22a)$$

$$a(x, t) \frac{\partial w_1}{\partial x} = -\frac{\partial w_0}{\partial t}, \quad w_1(\infty, t) = 0. \quad (22b)$$

³For $x > L, 0 < t \leq T$, the data a, b can be smoothly extended so that the problem (18b) is well defined over $\bar{\Omega}$ and the non-negativity of a, b is retained by their extensions.

These functions are used below to show that the solution u exhibits a boundary layer near $x = 0$. They satisfy

$$\left| \frac{\partial^{i+j} w_0}{\partial x^i \partial t^j}(x, t) \right| \leq C \varepsilon^{-i} e^{\frac{-x}{\varepsilon}}, \quad \left| \frac{\partial^{i+j} w_1}{\partial x^i \partial t^j}(x, t) \right| \leq C \varepsilon^{1-i} e^{\frac{-x}{\varepsilon}}, \quad 0 \leq i + j \leq 2.$$

We can decompose the solution into three distinct components

$$u(x, t) = v(x, t) + w(x, t) + z(x, t),$$

where w contains a boundary layer and z contains an interior layer. They are defined as the solutions of the problems:

$$Lv = 0, \quad (x, t) \in \Omega; \quad v(0, t) = u(0, t), \quad v(x, 0) = u(x, 0), \quad v \in C^2(\bar{\Omega}); \quad (23a)$$

$$Lw = f(x), \quad (x, t) \in \Omega; \quad w(0, t) = 0, \quad w(x, 0) = w_0(x, 0) - w_0(0, 0); \quad (23b)$$

$$Lz = 0, \quad (x, t) \in \Omega; \quad z(0, t) = 0, \quad z(x, 0) = -w(x, 0). \quad (23c)$$

Note that the initial condition for the component w is equivalent to

$$a(x, 0) \frac{\partial w}{\partial x}(x, 0) = f(x).$$

In addition, the interior layer component z is given by

$$z(x, t) = \begin{cases} 0, & x \leq g(t; 0, 0), \\ w_0(0, t) - w_0(x - g(t), t), & x \geq g(t; 0, 0). \end{cases}$$

From (21a) $f(0) = f'(0) = 0$ and hence $w(0, 0) = w_x(0, 0) = w_{xx}(0, 0) = 0$. By (3), it follows that $w, z \in C^2(\bar{\Omega})$. A global approximation \bar{Z} to the solution of (23c) can be generated using the algorithm in Section 4, where $d = 0$. Note that this approximation is generated on a mesh, defined in the transformed coordinate system. We next establish bounds on the first and second derivatives of w .

Lemma 5. *There exists a function $\chi \in C^2(\bar{\Omega})$ such that the solution of (23b) satisfies the following bounds*

$$|w(x, t) - \chi(x, t)| \leq C e^{\frac{-x}{\varepsilon}}, \quad \left\| \frac{\partial^{i+j} \chi}{\partial x^i \partial t^j} \right\| \leq C, \quad i + j \leq 2; \quad (24a)$$

$$\left| \frac{\partial^{i+j} (w - \chi)}{\partial x^i \partial t^j}(x, t) \right| \leq C \varepsilon^{-i} e^{\frac{-x}{\varepsilon}}, \quad 0 \leq i + j \leq 2. \quad (24b)$$

Proof. Consider the functions w_0 and w_1 defined in (22). Define $\chi \in C^2(\bar{\Omega})$ to be

$$\chi(x, t) := (w - w_0 - w_1)(x, t), \quad (25)$$

which is the solution of the problem

$$L\chi = -\frac{\partial w_1}{\partial t}, \quad \chi(0, t) = -(w_0 + w_1)(0, t), \quad (26a)$$

$$\chi(x, 0) = -w_0(0, 0) - w_1(x, 0). \quad (26b)$$

Observe that,

$$\begin{aligned} \left| \frac{\partial^{i+j} L\chi(x, t)}{\partial x^i \partial t^j} \right| &= \left| \frac{\partial^{i+j+1} w_1(x, t)}{\partial x^i \partial t^{j+1}} \right| \leq C\varepsilon^{1-i} e^{-\frac{x}{\varepsilon}}, \quad 0 \leq i + j \leq 2; \\ \left| \frac{\partial^j \chi}{\partial t^j}(0, t) \right| &\leq C, \quad 0 \leq j \leq 2; \quad \left| \frac{\partial \chi}{\partial x}(x, 0) \right| \leq C \left| \frac{\partial w_1}{\partial x}(x, 0) \right| \leq C. \end{aligned}$$

Note also that

$$\frac{\partial^2 \chi}{\partial x^2}(x, 0) = -\frac{\partial^2 w_1}{\partial x^2}(x, 0) = \left(\frac{\partial}{\partial x} \left(\frac{1}{a} \right) \frac{\partial w_0}{\partial t} + \frac{1}{a} \frac{\partial}{\partial t} \left(\frac{f}{a} \right) \right)(x, 0).$$

If $a_t(0, 0) = 0$, then

$$\left| \frac{\partial^2 \chi}{\partial x^2}(x, 0) \right| \leq C + Cx|f(x)| \leq C.$$

Hence, bounding χ and its derivatives as in Lemma 2, we deduce that

$$\left\| \frac{\partial^{i+j} \chi}{\partial x^i \partial t^j} \right\| \leq C, \quad 0 \leq i + j \leq 2.$$

Estimates (24b) follow from the definition (25) of χ and the bounds on the derivatives for w_0 and w_1 . \square

Based on these bounds on the derivatives of w , we will use a Shishkin mesh in space and a uniform mesh in time, which we shall denote by Ω_{SU}^N . The space domain is $[0, L] = [0, \sigma] \cup [\sigma, L]$ with the transition point as

$$\sigma := \min \left\{ \frac{L}{2}, \varepsilon \ln N \right\}.$$

On this mesh, we use a classical upwinded finite difference operator. The discrete problem is: Find W such that

$$L^{N,M} W(x_i, t_j) = f(x_i), \quad (x_i, t_j) \in \Omega_{SU}^N; \quad (27a)$$

$$W(0, t_j) = 0, \quad t_j \geq 0; \quad a(x_i, 0) D_x^- W(x_i, 0) = f(x_i), \quad x_i > 0. \quad (27b)$$

This new scheme also satisfies a discrete comparison principle.

Theorem 3. *If W is the solution of (27) and w is the solution of (23b), then*

$$\|\bar{W} - w\| \leq CN^{-1}(\ln N)^2 + CM^{-1}.$$

Proof. In analogous fashion to the decomposition of w , the discrete function W can be decomposed into several components. Denote by W_0, W_1, X the discrete counterpart of w_0, w_1 and χ given in (22) and (26). These functions are defined as the solutions of the following discrete problems.

$$\begin{aligned} a(x_i, t_j) D_x^- W_0(x_i, t_j) &= f(x_i), \quad W_0(L, t_j) = 0; \\ a(x_i, t_j) D_x^- W_1(x_i, t_j) &= -D_t^- W_0(x_i, t_j), \quad W_1(L, t_j) = 0; \\ L^{N,M} X(x_i, t_j) &= -D_t^- W_1(x_i, t_j), \\ X(0, t_j) &= -(W_0 + W_1)(0, t_j), \quad X(x_i, 0) = -W_0(0, 0) - W_1(x_i, 0). \end{aligned}$$

By noting that $W(x_i, 0) = W_0(x_i, 0) - W_0(0, 0)$, we see that

$$W = W_0 + W_1 + X.$$

For any mesh function Z , if

$$D_x^- Z(x_i) = g(x_i), x_i < x_N, \quad Z(x_N) = g(x_N), \text{ then} \quad (28a)$$

$$Z(x_i) = g(x_N) - \sum_{n=i+1}^N h_n g(x_n). \quad (28b)$$

Observe also that

$$\frac{\partial}{\partial x} \left(\frac{\partial w_0}{\partial t} \right) (x, t) = f(x) \frac{\partial a^{-1}}{\partial t}, \quad \frac{\partial w_0}{\partial t} (\infty, t) = 0 \text{ and} \quad (29a)$$

$$D_x^- (D_t^- W_0)(x_i, t_j) = f(x_i) D_t^- (a^{-1}(x_i, t_j)), \quad D_t^- W_0(L, t_j) = 0. \quad (29b)$$

Hence, using (28), we deduce that

$$|W_0(x_i, t_j)|, |D_t^- W_0(x_i, t_j)|, |W_1(x_i, t_j)|, |D_t^- W_1(x_i, t_j)| \leq C e^{-\frac{x_i}{\epsilon}}.$$

Then, for W_n , $n = 0, 1$, outside the fine mesh, where $x_i \geq \sigma$, we have

$$\begin{aligned} |(W_n - w_n)(x_i, t_j)| &\leq |W_n(x_i, t_j)| + |w_n(x_i, t_j)| \leq CN^{-1}; \\ |D_t^- (W_n - w_n)(x_i, t_j)| &\leq |D_t^- W_n(x_i, t_j)| + C \left\| \frac{\partial w_n}{\partial t} (x_i, t) \right\| \leq CN^{-1}, \end{aligned}$$

and within the fine mesh, where $x_i < \sigma$,

$$\begin{aligned} |D_x^- (W_0 - w_0)(x_i, t_j)| &\leq C \left| D_x^- w_0 - \frac{\partial w_0}{\partial x} \right| \leq C \frac{h}{\epsilon^2} e^{-\frac{x_i}{\epsilon}}, \\ |(W_0 - w_0)(x_i, t_j)| &\leq C \sum_{n=i+1}^{N/2} \frac{h^2}{\epsilon^2} e^{-\frac{x_i}{\epsilon}} + CN^{-1} \leq CN^{-1} \ln N. \end{aligned}$$

Using (29) and repeating the argument, we get that for $x_i < \sigma$

$$|D_t^- (W_0 - w_0)(x_i, t_j)| \leq CN^{-1} \ln N + CM^{-1},$$

and then for $x_i < \sigma$

$$\begin{aligned} |(W_1 - w_1)(x_i, t_j)| &\leq CN^{-1} \ln N + CM^{-1}, \\ |D_t^- (W_1 - w_1)(x_i, t_j)| &\leq CN^{-1} \ln N + CM^{-1}. \end{aligned}$$

From all of these bounds, we can then deduce that

$$|(X - \chi)(x_i, t_j)| \leq CN^{-1} \ln N + CM^{-1}.$$

Combine all of these bounds together to establish the nodal error bound

$$|(W - w)(x_i, t_j)| \leq CN^{-1} (\ln N)^2 + CM^{-1}, \quad (x_i, t_j) \in \Omega_{SU}^N.$$

This can be extended to a global error bound as in Theorem 2. □

Theorem 4. *If W is the solution of (27), V and Z are the discrete approximations to v, z and $\bar{U} = \bar{V} + \bar{W} + \bar{Z}$, then*

$$\|\bar{U} - u\| \leq CN^{-1} (\ln N)^2 + CM^{-1}.$$

where u is the solution of (2), (3), (21).

Remark 4. In the case where $b(x, t) \neq 0$ and $f(x, t)$, we define w_0 as the solution of

$$a(x, t) \frac{\partial w_0}{\partial x} + b(x, t)w_0 = f(x, t), \quad w_0(\infty, t) = 0.$$

Then, the numerical method is given by

$$\begin{aligned} L^{N,M} W(x_i, t_j) &= f(x_i, t_j), \quad W(0, t_j) = 0, \quad t_j \geq 0 \\ (aD_x^- + bI)W(x_i, 0) &= f(x_i, 0), \quad x_i > 0. \end{aligned}$$

6 | NUMERICAL RESULTS

In this final section, we examine a problem which is motivated by a mathematical model of fluid-particle interaction in particle-laden flows.^{3–5} The numerical solution of the problem requires the use of the three algorithms described in Sections 3–5. Let us consider two-phase fluid flow composed of a continuously connected phase (e.g., a gas, the carrier phase) and a dispersed phase (e.g., small particles) in a one-dimensional duct. Assuming all the particles move at the same constant velocity u_p , the flow is incompressible, the pressure gradients and the viscous losses are negligible,³ we have the following model to determine the velocity of the fluid u , the temperature of the fluid T , the cumulative density of the particles N_p in the x direction and the temperature of the particles T_p :⁴

$$\begin{aligned} \frac{\partial u}{\partial t} + u \frac{\partial u}{\partial x} &= -\lambda S_p(u - u_p) \frac{\partial N_p}{\partial x}; \\ \frac{\partial T}{\partial t} + u \frac{\partial T}{\partial x} &= r S_p(T_p - T) \frac{\partial N_p}{\partial x} + \frac{1}{\rho C_p} \frac{\partial^2 (kT)}{\partial x^2}, \quad r := \frac{h}{\rho C_p}; \\ \frac{\partial N_p}{\partial t} + u_p \frac{\partial N_p}{\partial x} &= 0; \\ \frac{\partial T_p}{\partial t} + u_p \frac{\partial T_p}{\partial x} &= -r S_p(T_p - T) + F, \end{aligned}$$

where F may be a function of the problem variables and other physical parameters and denotes a heat source term. For example, if the particles are heated by radiation, then $F(\epsilon, \zeta, S_p, T_\infty, T_p) = \epsilon \zeta S_p (T_\infty^4 - T_p^4)$.

Assuming that the reference frame moves with the particles (i.e., $x \rightarrow x + u_p t$), that the thermal diffusivity is small and that $T_p \gg T$, so that $T_p - T$ can be assumed constant, then the equation for the fluid temperature is of the general form: Find $T(x, t)$ such that

$$T_t + \omega_0(x, t)T_x = \beta z_x, \quad (x, t) \in (0, L] \times (0, T_f]; \quad (30a)$$

$$T(0, t) = T_0, \quad t \geq 0, \quad T(x, 0) = \phi(x) := T_0 + A_0 e^{-\frac{(x-d_0)^2}{\mu}}, \quad 0 \leq x \leq L; \quad (30b)$$

$$z(x, t) = A_1 \tanh \left(\frac{x - d_1}{\varepsilon} \right). \quad (30c)$$

Around $x = d_0$, the temperature is higher at the initial time. There is also a concentration of particles located at $x = d_1 > d_0$ which will exchange energy with the fluid, increasing its temperature. Note that the parameter ε controls the thickness of the layer of particles. The extreme case of ε very small corresponds to a single layer of particles. As the numerical methods designed in this paper are parameter-uniform, the numerical approximations will converge to the true solution irrespective of how small $\varepsilon > 0$ is and their global pointwise accuracy only depends on the number of mesh elements used in the computations.

⁴The model parameters in the system correspond to a drag coefficient λ , a convection coefficient h , the surface of the particle S_p , the fluid density ρ , the specific heat capacity of the fluid C_p , the thermal diffusivity k , the thermal emissivity ϵ , the Stefan–Boltzmann constant ζ and the heat source temperature T_∞ .

In the case of the fluid temperature, if the velocity ω_0 is constant, we can write out the exact solution explicitly as

$$T(x, t) = \begin{cases} \phi(x - \omega_0 t) + \frac{\beta A_1}{\omega_0} \left(\tanh\left(\frac{x-d_1}{\varepsilon}\right) - \tanh\left(\frac{x-\omega_0 t-d_1}{\varepsilon}\right) \right), & x \geq \omega_0 t, \\ T_0 + \frac{\beta A_1}{\omega_0} \left(\tanh\left(\frac{x-d_1}{\varepsilon}\right) + \tanh\left(\frac{d_1}{\varepsilon}\right) \right), & x \leq \omega_0 t. \end{cases}$$

Here, we shall take a variable fluid velocity for the fluid temperature as

$$\omega_0(x, t) = 2 - \frac{x}{L} \geq 1. \quad (30d)$$

In our numerical experiments, we take the sample parameter values of

$$L = 10, T_f = 5, \beta = 1, A_0 = 50, A_1 = 10, \quad (30e)$$

$$\mu = \varepsilon/4, T_0 = 300, d_0 = 2, d_1 = 5. \quad (30f)$$

As the problem (30) is linear, we can split the solution as follows.

$$T(x, t) = T_0 + P(x, t) + R(x, t),$$

where P solves the problem

$$P_t + \omega_0 P_x = 0, (x, t) \in (0, L] \times (0, T_f]; \quad (31a)$$

$$P(0, t) = 0, t \geq 0, P(x, 0) = \phi(x) - T_0, 0 \leq x \leq L. \quad (31b)$$

The component P corresponds to the initial pulse at $x = d_0$ transported in time. To solve for P numerically, we align the mesh to the characteristic

$$\frac{dx}{dt} = \omega_0(x), x(0) = d_0,$$

and follow the algorithm in Section 4. Note that the regular component of P is a constant function which takes the value of 300; and so it is only necessary to numerically approximate the singular component of P with the scheme (20). The transition point is of the form

$$\min \left\{ \frac{d_0}{2}, \frac{d_1}{2}, \sqrt{\mu} \ln N \right\},$$

either side of $s = 0$, where $s = x - g(t; d_0, 0)$. The second temperature component R (coming from the presence of the particles at $x = d_1$) is the solution of

$$R_t + \omega_0 R_x = \beta z_x, (x, t) \in (0, L] \times (0, T_f]; \quad (32a)$$

$$R(0, t) = 0, t \geq 0, \quad R(x, 0) = 0, x \geq 0. \quad (32b)$$

An approximation to R is generated separately on $\Omega^- := (0, d_1] \times (0, T_f]$ and $\Omega^+ := (d_1, L] \times (0, T_f]$. As $z_x(d_1, 0) \neq 0$, we observe that $R \notin C^1(\bar{\Omega}^+)$. We use the fitted operator algorithm on the Shishkin mesh Ω_S^N (described in Section 3) to generate an approximation R^N to R on the domain $\bar{\Omega}^-$. Hence, $R^N(d_1, t_j) = \Psi(t_j)$ will be determined. Finally, over Ω^+ , we further subdivide $R = S + I$ where $S \in C^0(\bar{\Omega}^+) \setminus C^1(\bar{\Omega}^+)$

$$S_t + \omega_0 S_x = \beta z_x, (x, t) \in \Omega^+; \quad (33a)$$

$$S(d_1, t) = 0, t \geq 0, S(x, 0) = \beta \int_{s=d_1}^x \frac{z_x(s)}{\omega_0(s)} ds, d_1 \leq x \leq L, \quad (33b)$$

and $I \in C^1(\bar{\Omega}^+)$ is such that

$$I_t + \omega_0 I_x = 0, (x, t) \in \Omega^+ := (d_1, L] \times (0, T_f], \quad (34a)$$

$$I(d_1, t) = R(d_1, t), t \geq 0, \quad I(x, 0) = -S(x, 0), d_1 \leq x \leq L. \quad (34b)$$

To approximate S over Ω^+ , we use an upwind operator on the Shishkin mesh Ω_{SU}^N and follow the procedure in Section 5.

To approximate the final component I , we use a transformation as in Section 4 either side of the characteristic curve $x = g(t; d_1, 0)$, where $I = 0$ at all points along this curve. Consider the following two subdomains

$$\Omega_L^+ := \{(x, t) \in \Omega^+ \mid x < g(t; d_1, 0)\}, \quad \Omega_R^+ := \{(x, t) \in \Omega^+ \mid x > g(t; d_1, 0)\}$$

and the associated subproblems

$$\begin{aligned} I_t + \omega_0 I_x &= 0, (x, t) \in \Omega_L^+ \cup \Omega_R^+, \\ I(d_1, t) &= 0, t \geq 0, \quad I(x, 0) = -S(x, 0), 0 \leq x - d_1 \\ I(x, 0) &= 0, x - d_1 \geq 0, \quad I(0, t) = \Psi(t) := R(d_1, t), 0 \leq t. \end{aligned}$$

From Lemma 2, we note that $R(d_1, t) \leq Ce^{-\frac{\kappa t}{\epsilon}}$, $\omega_0(x, t) > \kappa$. An approximation to I over the subdomain Ω_R^+ is generated using the transformation $s = x - g(t; d_1, 0)$ and over the subdomain Ω_L^+ using the transformation $\tau = t - g^{-1}(x; d_1, 0)$. The numerical method described in Section 4 is then applied, with

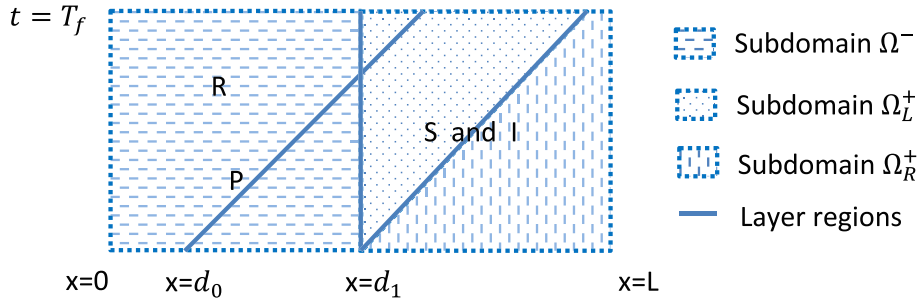


FIGURE 1 Layers regions, subdomains and components of the solution of Example (30) [Colour figure can be viewed at wileyonlinelibrary.com]

TABLE 1 Maximum and uniform two-mesh global differences and their corresponding orders of convergence for the component P (31)

	$N = M = 32$	$N = M = 64$	$N = M = 128$	$N = M = 256$	$N = M = 512$	$N = M = 1024$	$N = M = 2048$
$\epsilon = 2^0$	2.424E + 00	1.365E + 00	7.220E - 01	3.731E - 01	1.903E - 01	9.615E - 02	4.833E - 02
	0.829	0.919	0.952	0.971	0.985	0.992	
$\epsilon = 2^{-2}$	3.375E + 00	2.390E + 00	1.343E + 00	7.115E - 01	3.674E - 01	1.869E - 01	9.430E - 02
	0.498	0.831	0.917	0.954	0.975	0.987	
$\epsilon = 2^{-4}$	3.030E + 00	2.052E + 00	1.410E + 00	8.574E - 01	5.024E - 01	2.881E - 01	1.685E - 01
	0.562	0.542	0.717	0.771	0.802	0.773	
$\epsilon = 2^{-6}$	3.032E + 00	2.054E + 00	1.412E + 00	8.591E - 01	5.036E - 01	2.888E - 01	1.616E - 01
	0.562	0.541	0.717	0.771	0.802	0.837	
$\epsilon = 2^{-8}$	3.032E + 00	2.055E + 00	1.412E + 00	8.595E - 01	5.039E - 01	2.890E - 01	1.618E - 01
	0.561	0.541	0.716	0.770	0.802	0.837	
\vdots	\vdots	\vdots	\vdots	\vdots	\vdots	\vdots	\vdots
$\epsilon = 2^{-30}$	3.033E + 00	2.055E + 00	1.412E + 00	8.597E - 01	5.040E - 01	2.891E - 01	1.618E - 01
	0.561	0.541	0.716	0.770	0.802	0.837	
$D^{N,M}$	3.375E + 00	2.390E + 00	1.412E + 00	9.373E - 01	5.111E - 01	2.891E - 01	1.685E - 01
$P^{N,M}$	0.498	0.759	0.592	0.875	0.822	0.778	

Note: The numerical results have been obtained with the scheme (20).

$$\sigma_0 = \min \left\{ \frac{L}{2}, 2\varepsilon \ln N \right\} \quad \text{and} \quad \tau_0 = \min \left\{ \frac{T}{2}, 2\varepsilon \ln M \right\}.$$

Then, we form $\bar{R}^N = \bar{S}^N + \bar{I}^N$ over Ω^+ .

In the diagram of Figure 1, we identify the components P, R, S and I defined, respectively, in the subdomains $\bar{\Omega}, \bar{\Omega}^-, \bar{\Omega}^+$ and $\bar{\Omega}_L^+ \cup \bar{\Omega}_R^+$. All these components are used in our algorithm to approximate the fluid temperature T , which is the solution of (30).

In Tables 1–5, we give the maximum two-mesh global differences and the orders of convergence⁶ associated with the components P (in $\bar{\Omega}$), R (in $\bar{\Omega}^-$), S (in $\bar{\Omega}^+$), and I (in $\bar{\Omega}_L^+$ and $\bar{\Omega}_R^+$). Observe that the maximum two-mesh global differences in Table 1 for the component P are greater than the maximum two-mesh global differences in Tables 2–5, for the other components, due to the fact that the amplitude of the pulse is significantly larger than the amplitudes of the other components. The numerical results are only shown for the values of $\varepsilon = 2^0, 2^{-2}, 2^{-4}, 2^{-6}$, and 2^{-30} , but the uniform two-mesh global differences $D^{N,M}$ and the uniform orders of convergence $P^{N,M}$ are given in the last row of each table taking $\varepsilon = 2^0, 2^{-2}, \dots, 2^{-30}$. These numerical results indicate that the numerical scheme converges globally and uniformly with almost first order for all the components in agreement with the theoretical error bounds established in Sections 3–5.

TABLE 2 Maximum and uniform two-mesh global differences and their corresponding orders of convergence for the component R (32) in the subdomain $\bar{\Omega}^-$

	$N = M = 32$	$N = M = 64$	$N = M = 128$	$N = M = 256$	$N = M = 512$	$N = M = 1024$	$N = M = 2048$
$\varepsilon = 2^0$	2.597E – 01 0.938	1.356E – 01 0.867	7.431E – 02 0.924	3.916E – 02 0.958	2.016E – 02 0.978	1.024E – 02 0.989	5.159E – 03
$\varepsilon = 2^{-2}$	2.928E – 01 0.692	1.812E – 01 0.706	1.111E – 01 0.707	6.804E – 02 0.784	3.952E – 02 0.799	2.272E – 02 0.833	1.276E – 02
$\varepsilon = 2^{-4}$	2.962E – 01 0.700	1.824E – 01 0.720	1.107E – 01 0.740	6.631E – 02 0.734	3.988E – 02 0.818	2.262E – 02 0.833	1.270E – 02
$\varepsilon = 2^{-6}$	2.960E – 01 0.697	1.826E – 01 0.746	1.089E – 01 0.685	6.774E – 02 0.785	3.932E – 02 0.788	2.277E – 02 0.844	1.268E – 02
$\varepsilon = 2^{-8}$	2.960E – 01 0.697	1.826E – 01 0.723	1.106E – 01 0.740	6.624E – 02 0.734	3.983E – 02 0.818	2.259E – 02 0.833	1.268E – 02
\vdots	\vdots	\vdots	\vdots	\vdots	\vdots	\vdots	\vdots
$\varepsilon = 2^{-30}$	2.959E – 01 0.695	1.828E – 01 0.724	1.107E – 01 0.707	6.777E – 02 0.807	3.874E – 02 0.822	2.192E – 02 0.773	1.282E – 02
$D^{N,M}$	2.962E – 01	1.828E – 01	1.226E – 01	6.884E – 02	3.995E – 02	2.323E – 02	1.381E – 02
$P^{N,M}$	0.697	0.576	0.832	0.785	0.782	0.751	

Note: The numerical results have been obtained with the scheme (13).

TABLE 3 Maximum and uniform two-mesh global differences and their corresponding orders of convergence for the component S (33) in the subdomain $\bar{\Omega}^+$

	$N = M = 32$	$N = M = 64$	$N = M = 128$	$N = M = 256$	$N = M = 512$	$N = M = 1024$	$N = M = 2048$
$\varepsilon = 2^0$	2.610E – 01 1.002	1.303E – 01 1.001	6.513E – 02 1.000	3.255E – 02 1.000	1.627E – 02 1.000	8.136E – 03 1.000	4.068E – 03
$\varepsilon = 2^{-2}$	2.950E – 01 0.701	1.815E – 01 0.743	1.085E – 01 0.779	6.320E – 02 0.808	3.611E – 02 0.830	2.031E – 02 0.848	1.128E – 02
$\varepsilon = 2^{-4}$	2.967E – 01 0.699	1.827E – 01 0.748	1.088E – 01 0.782	6.326E – 02 0.809	3.611E – 02 0.830	2.031E – 02 0.848	1.128E – 02
$\varepsilon = 2^{-6}$	2.964E – 01 0.699	1.826E – 01 0.746	1.089E – 01 0.782	6.333E – 02 0.810	3.613E – 02 0.831	2.031E – 02 0.848	1.128E – 02
\vdots	\vdots	\vdots	\vdots	\vdots	\vdots	\vdots	\vdots
$\varepsilon = 2^{-30}$	2.964E – 01 0.699	1.826E – 01 0.746	1.089E – 01 0.782	6.332E – 02 0.809	3.614E – 02 0.831	2.032E – 02 0.848	1.128E – 02
$D^{N,M}$	2.970E – 01	1.827E – 01	1.226E – 01	6.513E – 02	3.614E – 02	2.032E – 02	1.128E – 02
$P^{N,M}$	0.701	0.576	0.912	0.850	0.831	0.848	

Note: The numerical results have been obtained with the scheme (27).

TABLE 4 Maximum and uniform two-mesh global differences and their corresponding orders of convergence for the component I (34) in the subdomain $\bar{\Omega}_L^+$

	$N = M = 32$	$N = M = 64$	$N = M = 128$	$N = M = 256$	$N = M = 512$	$N = M = 1024$	$N = M = 2048$
$\varepsilon = 2^0$	2.597E - 01 0.938	1.356E - 01 0.867	7.431E - 02 0.924	3.916E - 02 0.958	2.016E - 02 0.978	1.024E - 02 0.989	5.159E - 03
$\varepsilon = 2^{-2}$	2.928E - 01 0.692	1.812E - 01 0.706	1.111E - 01 0.707	6.804E - 02 0.765	4.003E - 02 0.806	2.289E - 02 0.838	1.281E - 02
$\varepsilon = 2^{-4}$	2.962E - 01 0.700	1.824E - 01 0.720	1.107E - 01 0.707	6.780E - 02 0.766	3.988E - 02 0.807	2.279E - 02 0.838	1.275E - 02
$\varepsilon = 2^{-6}$	2.960E - 01 0.697	1.826E - 01 0.723	1.106E - 01 0.708	6.774E - 02 0.766	3.984E - 02 0.807	2.277E - 02 0.838	1.274E - 02
\vdots	\vdots	\vdots	\vdots	\vdots	\vdots	\vdots	\vdots
$\varepsilon = 2^{-30}$	2.960E - 01 0.697	1.826E - 01 0.723	1.106E - 01 0.708	6.772E - 02 0.766	3.983E - 02 0.807	2.276E - 02 0.838	1.273E - 02
$D^{N,M}$	2.962E - 01	1.826E - 01	1.226E - 01	6.884E - 02	4.003E - 02	2.289E - 02	1.281E - 02
$P^{N,M}$	0.698	0.575	0.832	0.782	0.806	0.838	

Note: The numerical results have been obtained with the scheme (A4).

TABLE 5 Maximum and uniform two-mesh global differences and their corresponding orders of convergence for the component I (34) in the subdomain $\bar{\Omega}_R^+$

	$N = M = 32$	$N = M = 64$	$N = M = 128$	$N = M = 256$	$N = M = 512$	$N = M = 1024$	$N = M = 2048$
$\varepsilon = 2^0$	3.133E - 01 0.969	1.600E - 01 0.982	8.101E - 02 0.989	4.081E - 02 0.994	2.049E - 02 0.997	1.026E - 02 0.998	5.138E - 03
$\varepsilon = 2^{-2}$	3.488E - 01 0.675	2.185E - 01 0.728	1.319E - 01 0.763	7.773E - 02 0.805	4.448E - 02 0.826	2.509E - 02 0.847	1.395E - 02
$\varepsilon = 2^{-4}$	3.492E - 01 0.673	2.190E - 01 0.727	1.323E - 01 0.761	7.807E - 02 0.805	4.469E - 02 0.826	2.520E - 02 0.847	1.401E - 02
$\varepsilon = 2^{-6}$	3.494E - 01 0.672	2.192E - 01 0.726	1.325E - 01 0.761	7.819E - 02 0.805	4.476E - 02 0.826	2.525E - 02 0.847	1.403E - 02
\vdots	\vdots	\vdots	\vdots	\vdots	\vdots	\vdots	\vdots
$\varepsilon = 2^{-30}$	3.494E - 01 0.672	2.193E - 01 0.726	1.326E - 01 0.761	7.823E - 02 0.805	4.479E - 02 0.826	2.526E - 02 0.847	1.404E - 02
$D^{N,M}$	3.494E - 01	2.193E - 01	1.480E - 01	7.992E - 02	4.479E - 02	2.526E - 02	1.404E - 02
$P^{N,M}$	0.672	0.567	0.889	0.835	0.826	0.847	

Note: The numerical results have been obtained with the scheme (20).

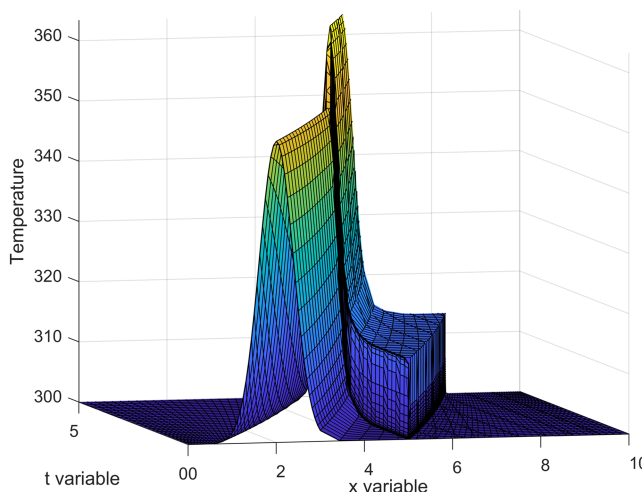


FIGURE 2 Example (30) with $\varepsilon = 2^{-8}$: Computed solution with $N = M = 64$ [Colour figure can be viewed at wileyonlinelibrary.com]

The numerical solution for Example (30) with $\epsilon = 2^{-8}$ is displayed in Figure 2 after patching the approximations computed for each one of the components of T . In this figure it is observed that the pulse in the initial condition is transported along the characteristic emanating from the point $(2, 0)$ and it merges with the interior layer located at $x = 5$. This interior layer is produced by the heat exchange from the particles to the gaseous phase. In addition, another interior layer emanating from the point $(5, 0)$ is observed. A physical explanation for this is that the initial condition for the temperature is not under equilibrium at $x = 5$ (i.e., there is no temperature gradient at $[5, 0]$ that satisfies a steady solution of Equation (30). As the particles start heating the gaseous phase at the initial time, the latter increases the temperature while being transported downstream, as observed in the figure in the form of an interior layer emanating from $(5, 0)$.

7 | CONCLUSIONS

Three classes of first-order singularly perturbed transport equations are examined. Boundary and interior layers can arise in the solutions of these problems. Numerical methods are constructed and analysed for these problems incorporating piecewise-uniform Shishkin meshes, which insert a significant proportion of the mesh points into the layer regions. In this way, the numerical methods produce parameter-uniform numerical approximations, whose global pointwise accuracy is guaranteed for all possible values of the singular perturbation parameter. A test problem, motivated from modelling fluid-particle interaction, is used to illustrate the performance of these numerical methods.

ACKNOWLEDGEMENT

This research was partially supported by the Institute of Mathematics and Applications (IUMA), the projects PID2019-105979GB-I00 and PGC2018-094341-B-I00 and the Diputación General de Aragón (E24-17R).

CONFLICT OF INTEREST

The authors declare that there are no conflict of interests to this work.

ORCID

José Luis Gracia  <https://orcid.org/0000-0003-2538-9027>

Adrian Navas-Montilla  0000-0002-3465-6898

Eugene O'Riordan  0000-0002-2363-7181

REFERENCES

- Markowich PA, Ringhofer CA, Schmeiser C. *Semiconductor Equations*. Vienna: Springer-Verlag; 1990.
- Slemrod M, Sternberg N. Quasi-neutral limit for Euler-Poisson system. *J Nonlinear Sci.* 2001;11(3):193-209. doi:10.1007/s00332-001-0004-9
- Baranger C, Desvillettes L. Coupling Euler and Vlasov equations in the context of sprays: the local-in-time, classical solutions. *J Hyperbolic Differ Equ.* 2006;3(01):1-26. doi:10.1142/S0219891606000707
- Lagoutière F, Seguin N, Takahashi T. A simple 1D model of inviscid fluid-solid interaction. *J Differ Equ.* 2008;245(11):3503-3544. doi:10.1016/j.jde.2008.03.011
- Linberman MA, Ivanov MF, Kiverin AD. Radiation heat transfer in particle-laden gaseous flame: Flame acceleration and triggering detonation. *Acta Astronaut.* 2015;115:82-93. doi:10.1016/j.actaastro.2015.05.019
- Farrell PA, Hegarty AF, Miller JJH, O'Riordan E, Shishkin GI. *Robust Computational Techniques for Boundary Layers*: CRC Press; 2000.
- Shishkin GI. Difference scheme for an initial-boundary value problem for a singularly perturbed transport equation. *Comput Math Math Phys.* 2017;57(11):1789-1795. doi:10.1134/S0965542517110136
- O'Riordan E, Pickett ML. A parameter-uniform numerical method for a singularly perturbed two parameter elliptic problem. *Adv Comput Math.* 2011;35(1):57-82. doi:10.1007/s10444-010-9164-1
- O' Riordan E, Quinn E. Numerical method for a nonlinear singularly perturbed interior layer problem. In: Clavero C, Gracia J. L., Lisbona F.J., eds. *Proc. International Conference on Boundary and Interior Layers - Computational and Asymptotic Methods, BAIL 2010*, Lecture Notes in Computational Science and Engineering. Zaragoza: Springer; 2011:187-195.
- O' Riordan E, Quinn J. Parameter-uniform numerical methods for some singularly perturbed nonlinear initial value problems. *Numer Algorithms.* 2012;61(4):579-611.
- Shishkin GI. Limitations of adaptive mesh refinement techniques for singularly perturbed problems with a moving interior layer. *J Comput Appl Math.* 2004;166(1):267-280. doi:10.1016/j.cam.2003.09.022
- Bobisud L. Second order linear parabolic equations with a small parameter. *Arch Rat Mech Anal.* 1968;27:385-397. doi:10.1007/BF00251441

13. Stynes M, O'Riordan E. A uniformly convergent Galerkin method on a Shishkin mesh for a convection-diffusion problem. *J Math Anal Appl.* 1997;214(1):36-54. doi:10.1006/jmaa.1997.5581

How to cite this article: Gracia JL, Navas-Montilla A, O'Riordan E. Parameter-uniform numerical methods for singularly perturbed linear transport problems. *Math Meth Appl Sci.* 2022;1-22. doi:10.1002/mma.8446

APPENDIX A: FURTHER CONSIDERATIONS WHEN APPROXIMATING A PULSE PROBLEM

In Section 4, a numerical scheme is described where it is assumed that the convective coefficient a_x does not change sign and the pulse occurs at the initial condition. In this appendix, we describe an algorithm to approximate the problem transporting a pulse when either a_x does change sign or the pulse occurs in the boundary condition.

A.1 | General case where a_x may change sign

If, for some $t = t_j$, the derivative a_x does change sign for $x < g(t; d, 0)$ (or $x > g(t; d, 0)$), then the scheme (20) should not be used to generate a numerical approximation to the singular component w . Observe that in this case the matrix associated with the scheme (20) is a reducible matrix.

In the case that a_x does change sign, for $s < 0$ (or $s > 0$), we would simply solve in the fine mesh region $[-\sigma_d, 0]$ (or $[0, \sigma_d]$) with the boundary value $\widetilde{W}(-\sigma_d, t_j) = 0$ (or $\widetilde{W}(\sigma_d, t_j) = 0$). That is, we would solve

$$\begin{aligned} D_t^- \widetilde{W} + [\tilde{a}(s_i, t_j) - \tilde{a}(0, t_j)] D_s^* \widetilde{W} + \widetilde{b} \widetilde{W} &= 0, \quad (s_i, t_j) \in (-\sigma_d, L-d) \times (0, T]; \\ \widetilde{W}(-\sigma_d, t_j) &= \widetilde{W}(L-d, t_j) = 0; \quad t_j > 0 \quad \widetilde{W}(s_i, 0) = \phi_2(s_i + d). \end{aligned}$$

Similarly to the case that a_x does not change sign, a global approximation \bar{W} to w is generated over the region $\bar{\Omega}$ and we set

$$\bar{W} \equiv 0 \text{ on } \bar{\Omega} \setminus \{(x, t), -\sigma_d + g(t; d, 0) \leq x \leq L, 0 \leq t \leq T\}.$$

A.2 | A pulse in the boundary condition

Consider problem (2), (3) with an ε -dependent boundary condition

$$u(0, t) = \psi_1(t) + \psi_2(t; \varepsilon); \tag{A1a}$$

$$\psi_2^{(j)}(0) = 0, \quad |\psi_2^{(j)}(t)| \leq C\varepsilon^{-j} e^{-\frac{|t-d|}{\varepsilon}}; \quad 0 \leq j \leq 2, \text{ if } 0 < d < T, \tag{A1b}$$

$$|\psi_2^{(j)}(t)| \leq Ct^\ell \varepsilon^{-(\ell+j)} e^{-\frac{t}{\varepsilon}}; \quad 0 \leq j \leq 2; \quad \ell \geq 3, \text{ if } d = 0. \tag{A1c}$$

The pulse in the boundary condition is transported along the characteristic curve $x = g_1(t; 0, d)$, which is the solution of the initial value problem

$$\frac{dx}{dt} = a(x, t), \quad x(d) = 0. \tag{A2}$$

To avoid excessive repetition, we outline the method only in the case for $d > 0$. The solution u can be decomposed into the sum of a regular component $v \in C^2(\bar{\Omega})$ and a layer component $w \in C^2(\bar{\Omega})$, defined as the solutions of

$$Lv = f, \quad (x, t) \in \Omega; \quad v(0, t) = \psi_1(t), \quad v(x, 0) = u(x, 0), \tag{A3a}$$

$$Lw = 0, \quad (x, t) \in \Omega; \quad w(0, t) = \psi_2(t; \varepsilon), \quad w(x, 0) = 0. \tag{A3b}$$

The non-singularly component v is approximated with a classical scheme on a uniform mesh. We examine now the singular component w . Note that $w(x, t) \equiv 0, x \geq g_1(t + d; d, 0)$. Consider the transformed variables, $\hat{u}(x, \tau) = u(x, t)$ where $\tau := t - g_1^{-1}(x; d, 0)$, then

$$\left[1 - \frac{\hat{a}(x, \tau)}{\hat{a}(x, 0)}\right] \hat{w}_\tau + \hat{a}\hat{w}_x + \hat{b}\hat{w} = 0, \quad \hat{w}(0, \tau) = \psi_2(\tau + d).$$

To generate a parameter-uniform approximation to w , solve the problem:

$$\left[1 - \frac{\hat{a}(x_i, \tau_j)}{\hat{a}(x_i, 0)}\right] D_\tau^* \hat{W} + \hat{a} D_x^- \hat{W} + \hat{b} \hat{W} = 0, \quad (x_i, \tau_j) \in \hat{S}_\sigma := (0, L] \times (-\sigma, \sigma); \quad (\text{A4a})$$

$$\hat{W}(x_i, -\sigma) = \hat{W}(x_i, \sigma) = 0; \quad \hat{W}(0, \tau_j) = \hat{\psi}_2(\tau_j). \quad (\text{A4b})$$

We form the global approximation $\bar{U} = \bar{V} + \bar{W}$ and

$$\|u - \bar{U}\| \leq CN^{-1} + CM^{-1}(\ln M)^2,$$

for the problem class (2), (3), (A1).